Exp. Theo. NANOTECHNOLOGY 10 (2026) 1285-1304 https://doi.org/10.56053/10.3.1285

Adsorption of Zn^{2+} ions using regenerated spent CoMo/γ-Al_2O_3 hydrodesulfurization catalyst

Aseel Jamal Ahmed[1,*], *Baraa Asaad Latoof*[2]

[1]Department of Chemistry, College of Science, University of Diyala, Baqubah, 32001 - Diyala, Iraq
[2]General Directorate of Education of Diyala, Baqubah, 32001 - Diyala, Iraq
[*]) Email: aseeljamal@uodiyala.edu.iq

Received 12/4/2026, *Received in revised form* 13/5/2026, *Accepted* 14/6/2026, *Published* 15/7/2026

Recycling of spent hydrodesulfurization (HDS) catalysts is viewed as an alternative approach to achieving sustainability objectives in environmental protection, particularly in waste management and water purification applications. Against this backdrop, the present research work focuses on the reusability of a spent CoMo/γ-Al_2O_3 HDS catalyst subjected to a set of operations that involve n-hexane solvent extraction of soluble carbon, an oxalic acid wash for foulant removal, and calcination at 500 ºC for 4 hours. The recovered catalyst is characterized via X-ray diffraction (XRD), Fourier-transform infrared spectroscopy (FTIR), and atomic force microscopy (AFM). The surface area is estimated using BET technique and found it to be 189.13 m^2/g. The obtained information reveals successful restoration, which is confirmed by the indicated crystal lattice parameters that correspond to a nanocrystallite size of roughly 2.03 nm. Batch experiments are conducted to test the ability of the restored catalyst in zinc ions (Zn^{2+}) adsorption from aqueous solution under different operating conditions. Results indicate that regeneration improves performance and reaches around 99% for the restored catalyst compared with 59% for the fresh sample. As the adsorbent dose and initial Zn^{2+} ion concentration is increased, the removal efficiency is increased; however, it is decreased with increasing temperature. The optimum adsorption capacity reaches 557.50, which is obtained at dose of 0.01 g, concentration of 120 ppm, pH of 6, time of 30 min, and temperature of 298 K. This is attributed to the exothermic nature of the process. Based on the system's thermodynamics, the obtained ΔG^o values are negative; this indicates that the process is spontaneous. Whereas negative ΔH^o and ΔS^o values indicate that the process is exothermic and associated with a decrease in randomness at the solid-liquid boundary.

Exp. Theo. NANOTECHNOLOGY 10 (2026) 1285-1304

Keywords: CoMo/γ-Al_2O_3 catalyst; Adsorption; Heavy metal removal, Wastewater treatment.

1. INTRODUCTION

Pollution is generally referred to as the substance that affects the environment by bringing about changes in the physical, chemical, and biological aspects. Pollution can be found in the air, in water bodies, or in the soil in different forms, depending on its nature, permanence, and strength [1]. Nanotechnology is an innovative branch of science that is involved in different remediation methods for reducing environmental pollution owing to unique characteristics such as a high specific surface area and high activity of the nanoscale materials [2]. Different kinds of nanoparticles (NPs) have been synthesized; they can be distinguished based on their unique structures including sphere-like, cylindrical or amorphous/crystalline type, and their size range is between 1 to 100nm [3]. Utilization of nanotechnology as enabling technology has made certain effects in different fields like environmental cleanup, energy, and chemicals [4].

Water has a significant role in the survival of living beings and in meeting basic human needs, such as domestic use, irrigation, and industrial operations [5]. However, pollution of water sources is a big issue nowadays for the environment and public health worldwide, especially in areas where water is unsafe to consume and the proper sanitation facilities are lacking [6,7]. It is known that water bodies may contain various pollutants like organic and inorganic compounds, metals, radioactive waste, and biological pollutants [8], where some could be detected by the naked eye and others could not. The presence of heavy metals (HMs) poses a threat due to their hazardous nature, longevity in the environment, non-degradable character, and ability to accumulate within organisms and the food chain [9-11]. HMs may originate from natural sources, but the huge increase in their concentrations is noticed after the Industrial Revolution. These could come from anthropogenic activities like mining, industrial effluents, agricultural operations, and garbage dumping [12-14].

Metal contamination poses substantial health hazards, which include cancer, kidney damage, bone disease, and heart-related illnesses [15]. While certain metals like zinc, copper, and nickel have roles within trace limits, excessive exposure could pose potential threats [16-18]. A variety of methods for treating metal pollutants like precipitation, ion-exchange process, solvent extraction, and membrane filtration are applied. But they may be expensive or ineffective where the concentrations are low [19,20]. Here, the importance of adsorption appears as one of the preferred methods due to its efficiency, simplicity, economy, and flexibility [21,22]. Some factors that affect the effectiveness of adsorption include pH, temperature, reaction time, concentration, and adsorbent characteristics [23]. The use of nanomaterials in adsorption could improve efficiency thanks to their high surface area and number of active sites [24].

Adsorption is defined as the adsorption of molecules or ions from the liquid or gaseous state and their deposition onto the surface of a solid adsorbent [25]. Being efficient and universal in its applications, the adsorption technique has been applied in various areas ranging from wastewater management to gas purification and industrial separation techniques [26-28]. Adsorption occurs through physical adsorption based mostly on intermolecular weak interactions or chemical adsorption relying on stronger binding interactions occurring at the surface of the adsorbent [29,30]. The spontaneity and type of adsorption can be characterized using thermodynamic values like Gibbs free energy change (ΔG^o), enthalpy change (ΔH^o), and entropy change (ΔS^o) [31-34].

The catalyst plays a crucial role in any process of industrial production. Specifically, the process of oil refining includes a series of catalytic reactions, which allow for transformations without consuming the catalysts [35]. The most common catalysts for desulfurization reactions include CoMo/γ-Al_2O_3 and NiMo/γ-Al_2O_3 catalysts, which are employed to eliminate sulfur impurities from petrochemical streams [36,37]. The broad usage of catalysts with a core of γ-Al_2O_3 is explained by their beneficial characteristics: large specific surface area, excellent thermal stability, and high mechanical strength [38-41]. Nevertheless, long-term use of catalysts in HDS results in the loss of catalytic activity due to the formation of coke layers, deposition of metallic elements, and sintering of the structure [42-45]. This leads to the generation of huge amounts of spent catalysts (from 150,000 to 170,000 tons annually) [46,47]. As spent catalysts contain valuable metals, such as cobalt, molybdenum, and nickel, they are reused through regeneration processes, which become important [48]. The thermal and chemical regeneration procedures help improve catalytic efficiency by eliminating coke and foulants [49,50]. Moreover, it should be noted that the reuse of spent hydro-processing catalysts is important because of the toxicity of metals released during their improper utilization [48].

There are many works in the literature on the treatment, regeneration, and reuse of wasted hydrodesulfurization catalysts. For instance, Abbas and Jung [51] have revealed that the oil residues on the spent HDS catalysts may be removed by solvent-assisted treatment and the catalyst support is recovered without substantial damage to its structure. Ahn et al. have suggested a remanufacturing process for used Ni–Mo/γ-Al_2O_3 catalysts using sequential oil washing, incineration, and acid leaching. This shows that the physicochemical qualities of the catalyst could be restored by removing carbonaceous deposits and metal impurities [52]. Similarly, Tian et al. show that the efficient removal of oil from spent HDS catalysts is an important pretreatment before further recovery or reuse, and that assisted cleaning procedures can increase the removal of petroleum residues [53]. Finally, Asencios and Sun-Kou demonstrated that high-surface-area γ-Al_2O_3 may adsorb hazardous metal ions, such as Zn(II), Cd(II) and Pb(II), from aqueous solutions in the context of adsorption applications [54]. However, the direct reuse of regenerated spent CoMo/γ-Al_2O_3 hydrodesulfurization catalyst as an adsorbent for Zn(II) removal from aqueous solution has not been paid much attention. Therefore, the present study is aimed to fill this gap through regeneration of the spent CoMo/γ-Al_2O_3 catalyst and studying its adsorption performance towards Zn^{2+} ions at varied operating settings.

The objective of this study is the investigation of the spent CoMo/γ-Al_2O_3 hydrodesulfurization catalyst regeneration process and assessment of its ability to absorb Zn^{2+} ions from aqueous media. The main objectives include the following: (i) regeneration of the spent CoMo/γ-Al_2O_3 catalyst through suitable physical and chemical regeneration processes; (ii) use of the regenerated CoMo/γ-Al_2O_3 catalyst for the absorption and removal of Zn^{2+} ions from aqueous media; (iii) determination of the optimal conditions, such as contact time, amount of the adsorbent, initial Zn^{2+} concentration, and temperature; and (iv) analysis of the thermodynamics of the Zn^{2+} ions absorption by the regenerated catalyst.

2. EXPERIMENTAL

2.1. Characterization techniques

The regenerated CoMo/γ-Al_2O_3 catalysts are analyzed using several methods. The crystal structure of the catalyst and the crystal size are evaluated by the use of X-ray diffraction technique (XRD). Scanning electron microscope (SEM; JEOL, Japan) is used to determine the surface morphology and particle structure of the catalysts. For identifying the functional groups and metal-oxygen interactions,

FTIR technique (Shimadzu IRPrestige-21, Japan) is used. Atomic Absorption (AA) Spectrophotometry technique (AAS; Shimadzu AA-7000, Japan) is used for evaluating the residual concentration of Zn^{2+} in the solution post-adsorption. Nitrogen gas adsorption-desorption is also carried out on the regenerated catalysts by using the Brunauer-Emmett-Teller (BET) technique.

2.2. Chemicals

The chemicals in this study are used as they are received. These are included zinc(II) chloride ($ZnCl_2$, 99%, molecular mass: 136.30 g/mol; Panreac, Spain) and absolute ethanol (C_2H_5OH, 99.9%, molecular mass: 46.07 g/mol; GCC). Also, n-hexane (C_6H_{14}, 99.8%, molecular mass: 86.18 g/mol; Sigma-Aldrich), and oxalic acid ($H_2C_2O_4$, 99.9%, molecular mass: 90.04 g/mol; Barcelona, Spain) are utilized. Zinc(II) chloride is used as the source of Zn^{2+} ions for aqueous solutions utilized in adsorption experiments. While n-hexane and oxalic acid are used during the regeneration treatment of the spent $CoMo/\gamma\text{-}Al_2O_3$ catalyst that is obtained from Aldora refinery, Baghdad, Iraq.

2.3. Preparation of solutions used in adsorption over HDS catalysts

A standard stock solution of Zn^{2+} ions is prepared by the dissolution of 2.0847 g of zinc(II) chloride ($ZnCl_2$) in deionized water, then diluting it to 1000 mL in a volumetric flask to obtain a concentration of 1000 mg L^{-1}. Zn^{2+} solutions with concentrations of 20, 40, 60, 80, 100, and 120 mg L^{-1} are then prepared by the dilution of the stock solution. Similarly, the 0.08 M oxalic acid ($H_2C_2O_4$) solution is prepared by dissolving 0.3600 g of oxalic acid in deionized water and diluting it to 50 mL.

2.4. Regeneration of spent catalysts

The spent catalyst, which is shaped mostly cylindrical (with different dimensions), has oil that is adhered to it. This is ground into a powder and sieved in a mesh with a size of 75 μm, so the particles size is equal or lower than this number. Figure 1 (A and B) shows the change in size before and after grinding, respectively. The catalyst particles are washed with distilled water in order to remove any impurities, then dried in an oven at 100 ºC for 2 hours. The dried catalyst go through a three-stage pre-treatment process. The textural properties of the regenerated $CoMo/\gamma\text{-}Al_2O_3$ catalyst are determined by nitrogen adsorption–desorption analysis using the BET method. Before analysis, the sample is degassed at 120 °C for 2 h to remove physically adsorbed moisture and impurities from the surface. The measurement is carried out by using N_2 as the adsorptive gas at 77 K. The BET method is applied to estimate the specific surface area, while the total pore volume is calculated from the adsorbed nitrogen amount at high relative pressure. The average pore diameter and pore-size distribution are determined using the BJH method.

(A) (B)

Figure 1 Spent CoMo/γ-Al_2O_3, (A) Before and (B) After grinding.

The regeneration process of the spent CoMo/γ-Al_2O_3 catalyst is accomplished through three stages, namely, solvent extraction, acid leaching, and heating. This entails placing 9 g of the spent catalyst in an extraction apparatus consisting of a round bottom flask fitted with a condenser for treatment with n-hexane refluxed at 75–85 ºC for 6 h at 200 rpm stirrer rate to extract soluble coke from the catalyst. This extracted solid is filtered and dried in a vacuum oven at 110 ºC for 3 h. In the next stage, 5 g of the n-hexane-extracted catalyst is leached with 50 mL of 0.08 M oxalic acid solution at 75–85 ºC for 1 h under stirring at 200 rpm for removal of foulants. After filtering and washing the catalyst repeatedly with distilled water, it is dried in a hot air oven at 150 ºC for 2 h before being is cooled in a desiccator. All the three (spent catalyst, n-hexane-treated catalyst, and oxalic acid/n-hexane treated catalysts) are calcined in a muffle furnace at 500 ºC for 4 h to decompose the insoluble coke present on the catalysts.

2.5. Factors affecting adsorption method

The effect of contact time on Zn^{2+} adsorption is investigated using batch experiments at 298 K. For the experiment, 50 mL of Zn^{2+} solution of 100 mg L^{-1} initial concentration and pH 6 is mixed with 0.10 g of the regenerated CoMo/γ-Al_2O_3 catalyst. The mixtures are agitated in capped vessels by employing a thermostatically controlled water-bath shaker that ran at 150 rpm. Samples are mixed at times of 10, 20, 30, 40, and 50 min, then filtered to remove suspended catalyst particles. The residual Zn^{2+} concentration in the filtrate is measured by the AAS.

The effect of adsorbent dose on Zn^{2+} removal is examined by applying different amounts of the regenerated catalyst. Doses of 0.01, 0.05, 0.10, 0.15, and 0.20 g are applied. The other factors are included the use of 50 mL of Zn^{2+} solution with an initial concentration of 100 mg L^{-1} at pH 6 and 298 K. The separation procedure is used as described above.

The influence of initial Zn^{2+} concentration is studied using 50 mL solutions of the concentrations 20, 40, 60, 80, 100, and 120 mg L^{-1}. The experiments are carried out using 0.15 g of the catalyst at pH 6, 298 K, a stirring rate of 150 rpm, and a fixed contact time of 30 min that is selected based on the equilibrium time determined in the contact-time study. Lastly, the effect of temperature is evaluated at 298, 308, 318, and 328 K. The experiments are performed using 50 mL of Zn^{2+} solution under the

selected conditions: pH 6, initial Zn^{2+} concentration of 100 mg L^{-1}, adsorbent dose of 0.15 g, stirring rate of 150 rpm, and contact time of 30 min.

The desorption process is carried out by initially adjusting the pH of the Zn^{2+} solutions to 6.0 ± 0.1 by micro-additions of 0.1 M HCl or 0.1 M NaOH solutions. The pH is measured with a digital pH meter calibrated with standard buffer solutions. In order to study the effect of pH on the adsorption process, it is adjusted by the mentioned solutions to achieve the desired value of pH.

2.6. Calculation of metal removal

The removal ratio (R%) of Zn^{2+} is calculated using the following equation [55,56].

$$R(\%) = (C_0\text{-}C_e)/ C_0 \times 100 \quad (1)$$

where: R %: The percentage metal removal; C_0: The initial concentration of metal ion (mg /L); and C_e: The equilibrium concentration of metal ion after adsorption at any time, mg L^{-1}.

The adsorbed Zn^{2+} on the adsorbent at equilibrium (q_e (mg/g)) is estimated by the following equation:

$$q_e = [(C_0 – C_e) \times V] / W \quad (2)$$

Where C_0 and Ce are mentioned above. V is volume of aqueous solution (L), and W is dry mass of regenerated catalyst (g).

3. RESULTS AND DISCUSSION

3.1. Characterization of regenerated (CoMo/γ-Al_2O_3) catalysts

3.1.1. X-ray diffraction

The crystalline phase composition of the prepared materials and the assessment of their crystal structure are determined using XRD. The results of the XRD of the three major diffraction peaks for the regenerated CoMo/γ-Al_2O_3 catalyst and the diffraction patterns of the regenerated catalyst are shown in Figure 2 and Table 1. The average particle size is calculated by using the Debye-Scherrer formula [57].

$$D = \frac{0.9\,\lambda}{\beta \cos\theta} \quad (3)$$

where D is the crystallite size, λ is the wavelength of radiation, θ is the Bragg's angle, and β is the full width at half maximum (FWHM).

The calculated value of the crystallite size for the regenerated catalyst CoMo/γ-Al_2O_3 is 2.028 nm. The appearance of sharp diffraction peaks in the X-ray diffractogram, along with a crystallite size of less than 100 nm, indicates that the synthesized product is a nanocrystal.

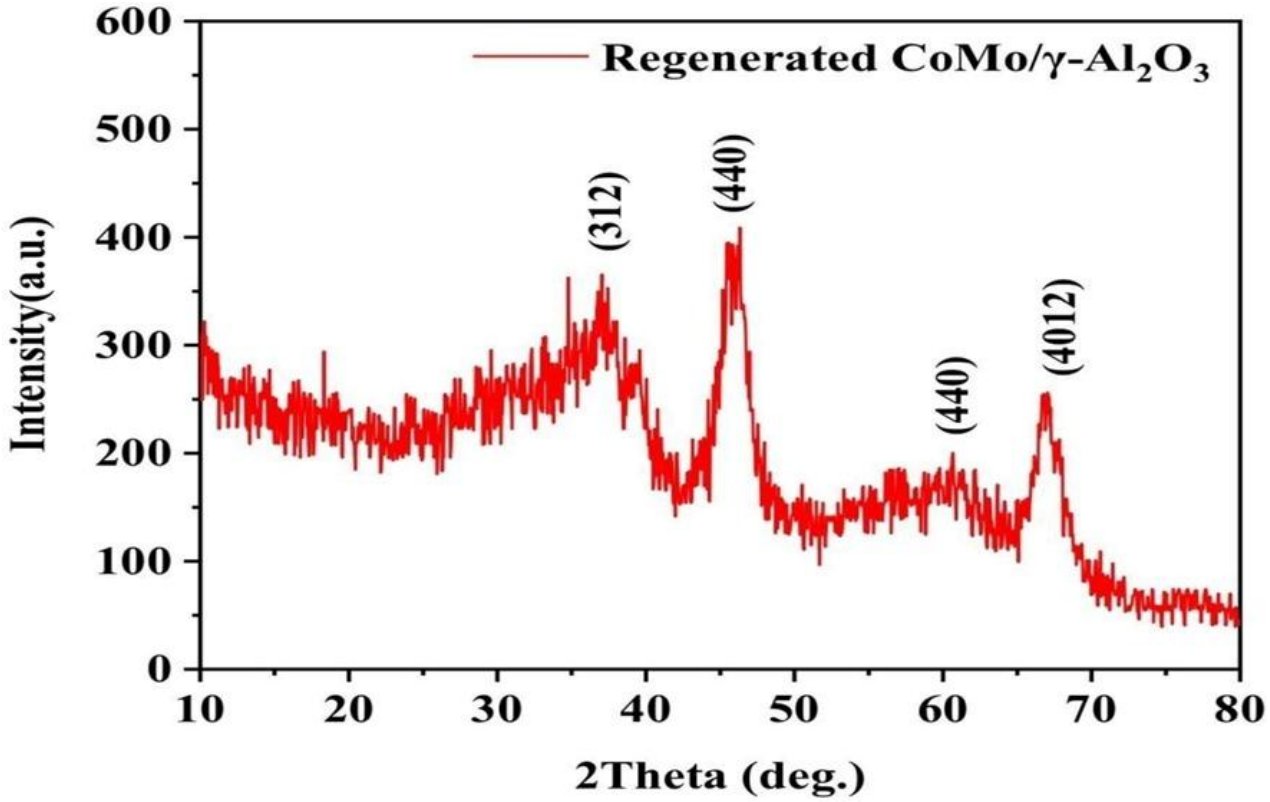

Figure 2 XRD of regenerated CoMo/γ-Al_2O_3.

Table 1 Structural characterizations of XRD.

Pos. [°2Th.]	Height [cts]	FWHM Left [°2Th.]	d-spacing [Å]	Rel. Int. [%]	Tip Width
37.8668	73.77	3.9360	2.37600	35.47	4.7232
45.6340	207.95	1.7712	1.98803	100.00	2.1254
58.7040	51.10	4.7232	1.57278	24.57	5.6678
67.0393	158.28	1.5744	1.39606	76.11	1.8893

3.1.2. FTIR Spectra Analysis

The FTIR spectrum of the regenerated catalyst is shown in Figure 3. The absorption peaks that are detected between 400 and 1050 cm^{-1} could be linked to the vibrations of metal-oxygen species. The peak is seen at 895.08 cm^{-1} could be related to MoO_3 species, while those are recorded at 667.00 cm^{-1} and 429.91 cm^{-1} represent the vibrational spectra of Al-O species [58, 59]. These could be considered as a sign of the presence of aluminum atoms in octahedral and tetrahedral structures, respectively. This observation is in agreement with the FTIR spectra of CoMo/γ-Al_2O_3 catalyst.

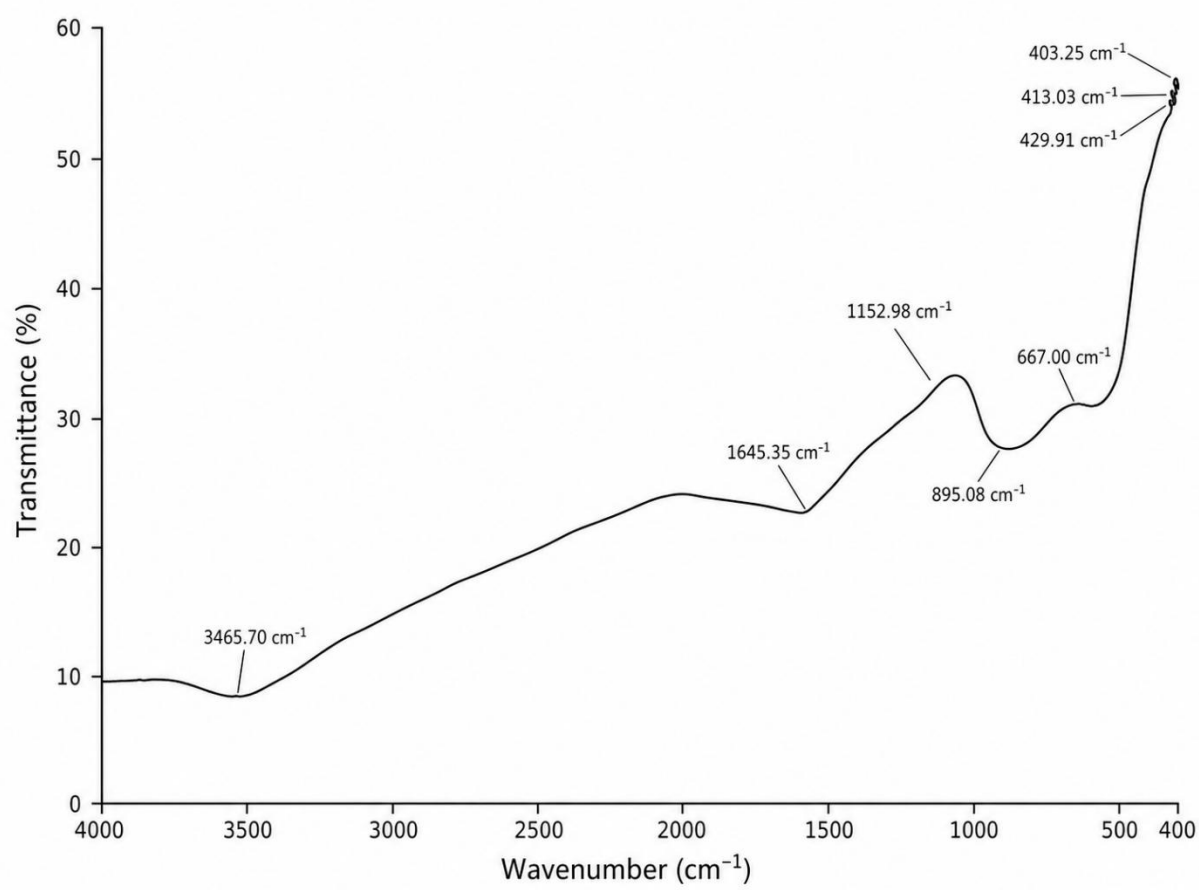

Figure 3 FTIR spectrum of regenerated CoMo/γ-Al_2O_3 catalyst.

3.1.3. Scanning electron microscope test

The SEM technique is utilized to check and analyze the morphological merits of the samples [60, 61]. Figure 4 shows SEM images of the reformed CoMo/γ-Al_2O_3 catalyst, revealing irregular, partially spherical particles. The mean particle size is 27.86 nm.

The particle/grain size obtained from SEM is compared with the crystallite size calculated from XRD analysis. The XRD-based crystallite size of the regenerated CoMo/γ-Al_2O_3 catalyst is approximately 2.028 nm, whereas the SEM image shows an average grain size of about 27.86 nm. This difference is reasonable because XRD peak broadening estimates the coherent crystalline domain size, whereas electron microscopy measures the apparent particle or grain size, which may consist of aggregated crystallites [62]. Therefore, the larger SEM grain size suggests that the visible grains are composed of several smaller crystallites aggregated together after regeneration and calcination.

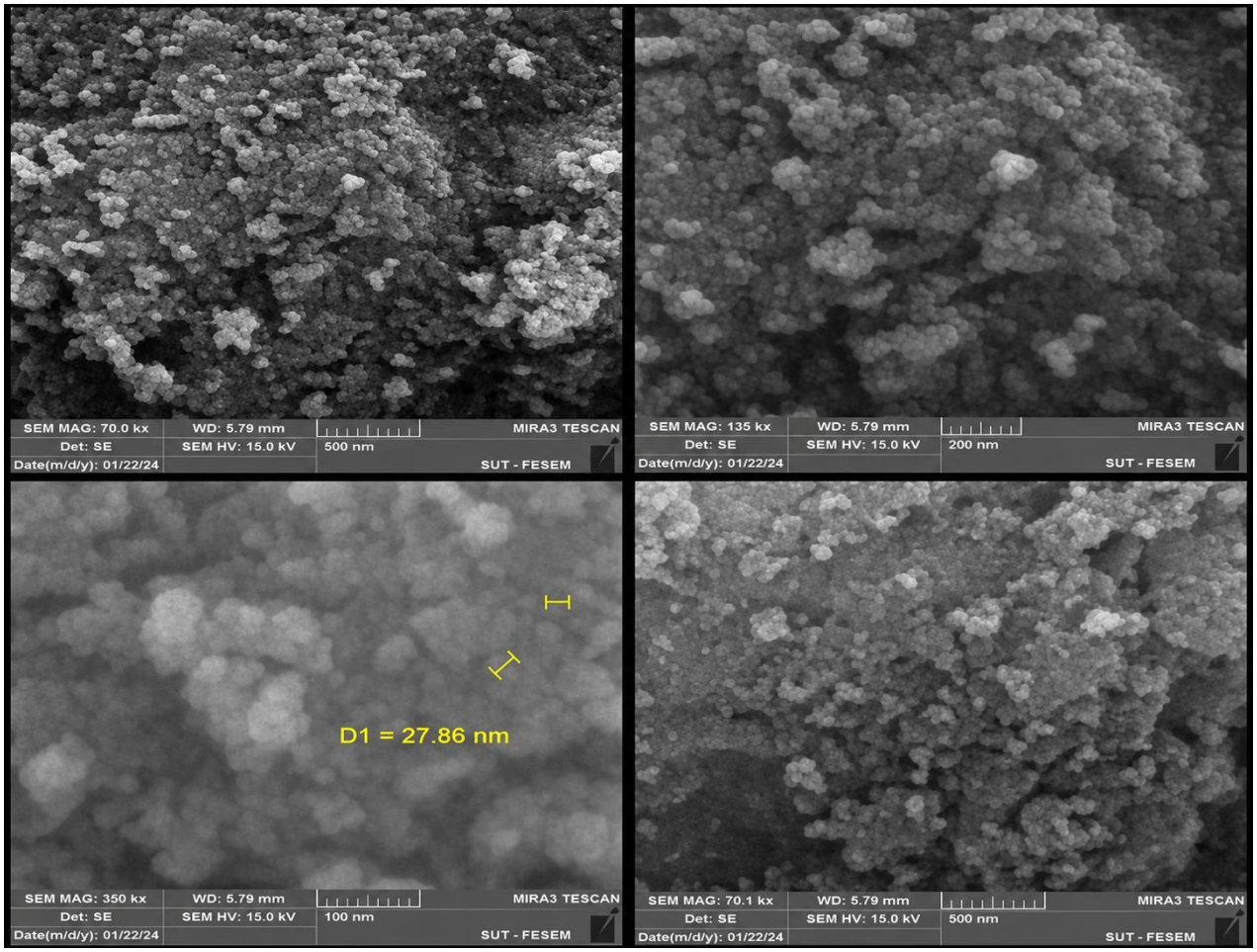

Figure 4 SEM images of regenerated CoMo/γ-Al_2O_3 NPs.

3.1.4 Structural characteristics

The BET result shows that the regenerated catalyst is highly porous. The specific surface area is found to be 189.13 m^2/g, while the pore volume and diameter are determined as 0.4905 cm^3/g and 10.374 nm, respectively. Yet, the pore volume by BJH is reported to be 0.5084 cm^3/g whereas the pore diameter is 9.30 nm. Findings suggest a mesoporosity structure with pore diameters falling within the range of 2 to 50 nm. High surface area and accessibility of mesopores promote the diffusion of Zn^{2+} ions and provide numerous active sites, which result in high adsorption capacity during the adsorption study. It is good to mention that the found diameter value is different than the SEM images findings, but both fall within the same range of mesoporosity structure.

3.2. Regeneration of spent CoMo/γAl_2O_3 catalysts

The regeneration results are listed in Table 2, they show that the used catalyst had about 8.8027 wt.% soluble coke, which is stripped by n-hexane. Furthermore, the main contaminant metals (Fe, Ca, As, and sulfates), which make up 11.6 wt.% of all contaminants, are effectively terminated using oxalic acid. Insoluble coke, making up 18.00 wt.% of all contaminant materials, is cleaned through

calcination. Regeneration helped improve some of the physicochemical properties of the catalyst, such as the reconstitution of the active metal ions, nickel, and molybdenum, as well as γ-Al_2O_3 support. Regeneration is assumed to improve the surface properties that are altered due to detrimental sintering and fouling during the previous use. This greatly improves the adsorption efficiency of the catalyst. Thus, the regenerated catalyst has an ability to remove Zn^{2+} ions of about 99%, whereas the used catalyst only has about 59%.

Table 2 Physical and chemical properties of commercial, spent, and regenerated $CoMo/\gamma Al_2O_3$ catalysts.

Property	New	Spent	Regenerated
CoO	4.10 wt.%	2.27 wt.%	3.03
MoO_3	12.90 wt.%	11.36 wt.%	15.15
Al_2O_3	81.00 wt.%	61.35 wt.%	81.82
Na_2O	< 0.04	With foulant	0.0
Fe	< 0.08		0.0
SiO_2	< 0.24		0.0
Soluble coke	0.0	8.80	0.0
Insoluble coke	0.0	11.6	0.0
Fouling elements, Fe, Ca, As	0.0	18	0.0
Normal size	1.5-2.5 mm	< 1.5-2.5 mm	< 1.5-2.5 mm
Form	Extrudates	Extrudates	Powder

3.3. Adsorption of Zn^{2+} ions on regenerated $CoMo/\gamma Al_2O_3$ catalysts

The concentration of Zn^{2+} ions is determined using AAS. The absorbance of Zn^{2+} solutions is measured at a maximum wavelength (λ_{max}) of 213.9 nm. The following sections denote the obtained results.

3.3.1. Adsorption of Zn^{2+} ions on spent $CoMo/\gamma$-Al_2O_3 catalyst

Removal of Zn^{2+} ions from aqueous solutions by the spent $CoMo/\gamma$-Al_2O_3 catalyst is studied under the following experimental conditions: initial metal ion concentration of 100 mg/L, pH 6, adsorbent dose 0.15 g, temperature 298 K, and contact time 30 min. An efficiency of 59% removal is obtained (as mentioned previously).

3.3.2. Effect of contact time on adsorption

The impact of contact time on the adsorption of Zn^{2+} by the regenerated CoMo/γ-Al_2O_3 catalyst is analyzed at different times of 10, 20, 30, 40, and 50 minutes while maintaining temperature (298 K), Zn^{2+} concentration (100 mg L^{-1}), pH (6), and dose (0.1 g) the same. The relation between removal efficiency and contact time is provided in Figure 5. Based on the data, it can be concluded that equilibrium is attained in approximately 30 min for Zn^{2+} adsorption by the regenerated catalyst, after which no further notable changes are observed.

This is due to the relatively high number of active adsorption sites at the onset of the process and to the large concentration difference between the solution and the adsorbent surface. The decreasing number of adsorption sites reduces the rate of adsorption toward equilibrium. Equilibrium is attained as there are no more active adsorption sites [63]. Moreover, the rapid initial uptake indicates a highly dynamic process, where the majority of Zn^{2+} ions are removed in the first 20 min due to the direct access of unoccupied functional groups on the outer surface of the catalyst. As these surface sites are gradually filled, the adsorbed ions began to generate electrostatic repulsion, which are hindered further adsorption. The remaining ions have to slowly diffuse into the internal pores until the monolayer saturation is reached. From a practical and industrial point of view, the fast attainment of equilibrium within a 30 min time frame indicates the successful recovery of the surface-active sites of the catalyst by the regeneration. Moreover, the determination of such optimum residence time is an important parameter for limiting the energy consumption of agitation and thus to decrease the total operational cost of the water treatment process [64-66].

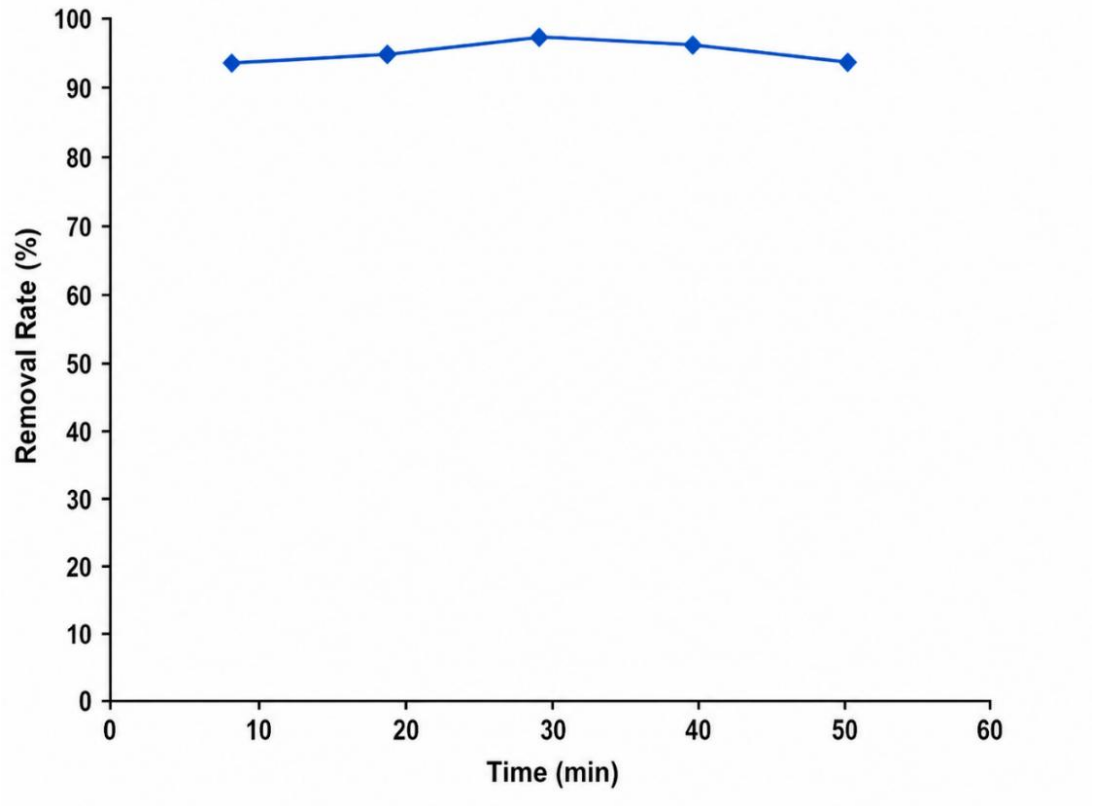

Figure 5 Effect of contact time on Zn^{2+} ion removal on the regenerated CoMo/γ-Al_2O_3 catalyst.

3.3.3. Effect of adsorbent quantity on adsorption

Adsorbent dose effects on the removal of Zn^{2+} Ions. Adsorbent dose effects on Zn^{2+} ions have been studied by changing the mass of regenerated CoMo/γ-Al_2O_3 in the range of 0.01, 0.05, 0.10, 0.15, and 0.20 g at constant temperatures of 298 K, initial concentration of 100 mg L^{-1}, pH value of 6, and fixed contact time of 30 min. The impact of changes in the adsorbent dosage on the Zn^{2+} ions removal is presented in Figure 6. It can be observed that an increase in adsorbent dosage causes more Zn^{2+} ions to be adsorbed. The reason could be explained by the provision of more adsorption sites through an increase in the adsorbent dose [67]. This improvement is directly related to the increased total surface area and the relative increase in the number of vacant active functional groups, which increases the collision probability between the Zn^{2+} cations and the available binding sites. Yet, it is generally observed that beyond a certain optimal dosage, the marginal increase in removal efficiency levels off or even declines. This is because, at the higher adsorbent doses, the total number of adsorption sites available is much higher than the fixed metal ions concentration available in the bulk solution and hence many active sites remain unoccupied [68]. In addition, high adsorbent concentrations can cause particle aggregation or overlapping in the solution, which effectively masks and reduces the available surface area. Split-level concentration gradients at high doses can further contribute to the reduction in specific adsorption capacity (qe). From the process optimization point of view, it is important to determine the inflection point where the maximum efficiency meets the minimum mass consumption to guarantee an economically viable and cost-effective water purification operation [67,68].

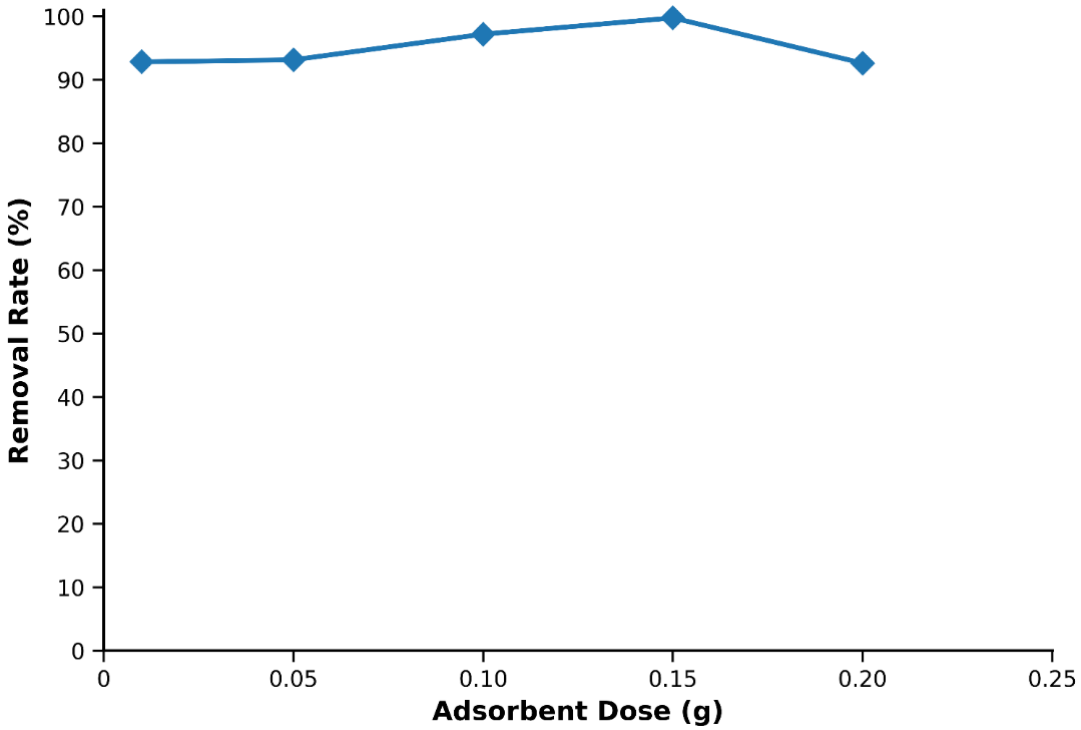

Figure 6 Effect of adsorbent quantity on the removal rate of Zn^{2+} ions.

3.3.4. Effect of initial concentration of Zn^{2+} on adsorption

The impact of the initial Zn^{2+} concentration on adsorption is studied at concentrations of 40, 60, 80, 100, and 120 mg L^{-1}. The results are illustrated in Figure 7; the indicated that the removal ratio of zinc ions decreased as the initial concentration increased. This behavior could be attributed to the limited number of active adsorption centers on the catalyst surface. With fewer zinc ions in solution, more centers become occupied; thus, the removal increased. In contrast, when the initial concentration of ions rose, the available number of adsorption sites are saturated. Moreover, while a larger concentration difference initially leads to better mass transfer, it eventually saturates and results in no extra absorption [52]. This inverse relationship between the removal ratio and the initial concentration is a characteristic feature of batch adsorption systems operating with a fixed mass of adsorbent. At lower concentrations, the ratio of the available surface area and the vacant functional groups to the total number of Zn^{2+} ions in the bulk solution is extremely high, allowing almost all present ions to find an active site easily. Conversely, at higher initial concentrations, the fixed quantity of active centers becomes the limiting factor. The competitive interaction among the excessive number of Zn^{2+} cations for the remaining crowded sites intensifies, leaving a substantial fraction of the metal ions unabsorbed in the solution. This plateau effect confirms that the active sites are completely surface-covered, shifting the process from being controlled by mass-transfer resistance to being limited by the specific adsorption capacity of the regenerated catalyst [52,67].

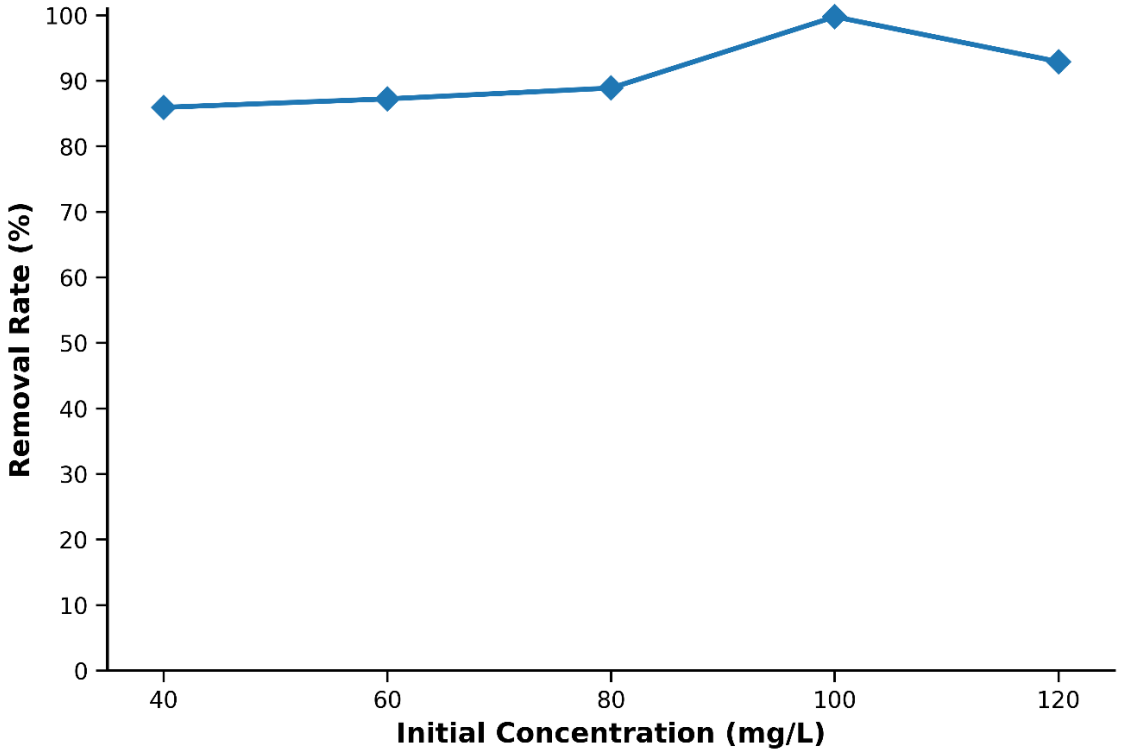

Figure 7 Effect of initial concentration on the removal of Zn^{2+} ions.

3.3.5. Effect of temperature on adsorption

The influence of temperature on Zn^{2+} adsorption is studied at 298, 308, 318, 328, and 338 K, while the other parameters are set as pH = 6, initial concentration = 100 mg L^{-1}, amount of adsorbent = 0.15 g, and contact time = 30 min. The results are presented in Figure 8. From the figure, it is clear that the removal ratio is decreased by increasing temperature. This implies that the adsorption process is exothermic. The reduction in adsorption capacity may be due to weakened interactions between Zn^{2+} ions and the active sites of the regenerated catalyst. Also, as the temperature rose, the thermal energy could increase and lead to a desorption from the surface. The exothermic nature shows that the operational performance is thermodynamically favorable at low temperatures. At elevated temperatures, the additional thermal energy supplied to the system increases the kinetic energy of the adsorbed Zn^{2+} ions, thus increasing their mobility and their ability to overcome the attractive forces that hold them to the catalyst surface. This in turn causes a shift in the adsorption-desorption equilibrium toward the desorption phase. Moreover, the physical structural integrity of the active functional groups or the binding sites on the regenerated CoMo/γ-Al_2O_3 matrix might be subjected to subtle thermal distortions or weakening at higher temperatures thus reducing their affinity for metal cations. This trend indicates that the attachment mechanism is dominated by physical forces or weak chemical interactions, since true chemisorption should exhibit the opposite trend with increasing temperature.

The temperature range is confined to 298-338 K as the adsorption studies are carried out in aqueous solution at atmospheric pressure. Increasing the temperature above 400 K would lead to large water evaporation and a pressurized system, which is not the case in practical wastewater-treatment circumstances. Therefore, the chosen temperature range is adequate to study the influence of temperature on Zn^{2+} adsorption. After exploring all of the conditions, it can be stated that the maximum adsorption capacity attained is 557.50, achieved at a dosage of 0.01 g, a concentration of 120 ppm, a pH of 6, a time of 30 min, and a temperature of 298 K.

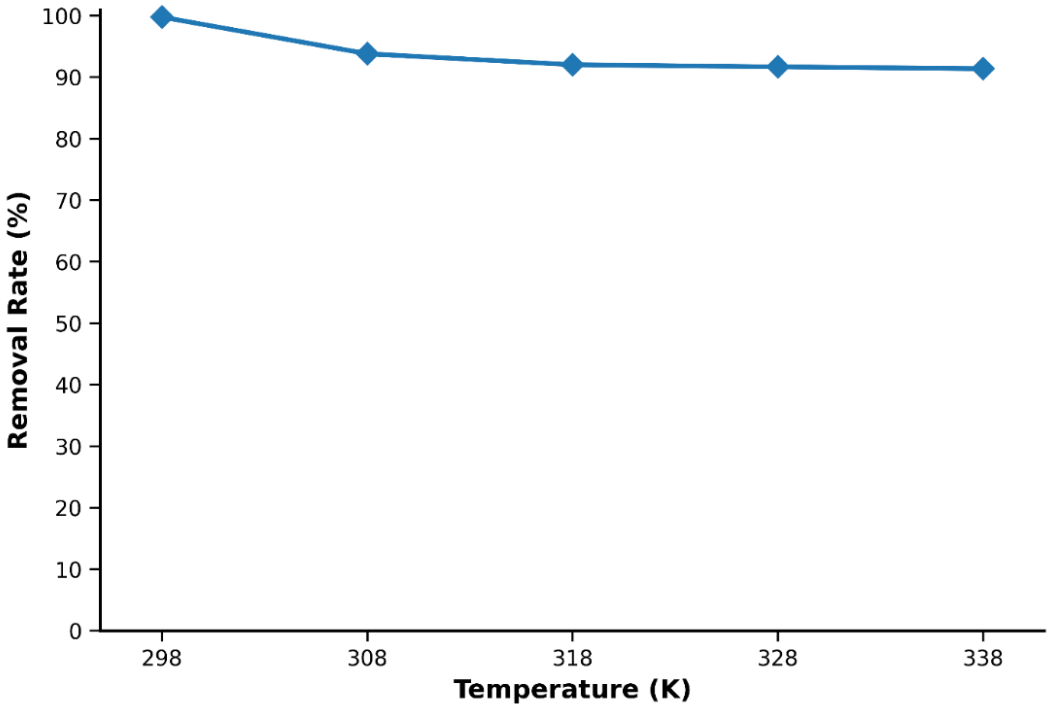

Figure 8 Effect of temperature on the removal rate.

3.4. Thermodynamic study of CoMo catalysts

The effects of temperature on the adsorption of Zn^{2+} by regenerated CoMo/γ-Al_2O_3 are studied at 298, 308, 318, 328, and 338 K. The aim is to obtain the thermodynamic constants for the adsorption process in terms of the standard Gibbs free energy (ΔGº), enthalpy (ΔHº), and entropy (ΔSº). The adsorption equilibrium constant (K) is obtained from the Van't Hoff equation as described below:

$$\ln K = -\frac{\Delta H}{R}\left(\frac{1}{T}\right)\frac{\Delta S}{R} \quad (4)$$

The equilibrium constant (K) at different temperatures was calculated by equation 5:

$$K=\frac{Qe \times m(g)}{Ce \times V\ (L)} \quad (5)$$

Where Q_e: The adsorption capacity of metal ions (mg/g), m: The mass of the catalysts (g), C_e: The concentration at equilibrium after Zn^{2+} removal (mg/L), and V: Volume of the aqueous solution (L).

Table 3 presents the equilibrium constant (K) values for the adsorption of Zn^{2+} ions onto the regenerated CoMo/γ-Al_2O_3 at different temperatures. The standard Gibbs free energy change (ΔG^o) is calculated by the following equation [69]:

$$\Delta G^o = - RT \ln k \quad (6)$$

in which $\Delta G°$ is the standard free energy change (kJ/mole), R the gas constant (8.314×10^{-3} kJ/mol.K), T the absolute temperature (K), and k the equilibrium constant. Figure 9 shows Van't Hoff Plot for adsorption of Zn^{2+} ions on regenerated CoMo/γ-Al_2O_3 catalyst. Finally, the values of (ΔH^o) and (ΔS^o) can be calculated from the slope and intercept of the plot (lnk) versus (1/T) [70,71] as explained by equations:

$$\text{Slope} = - \Delta H/R \quad (7)$$

$$\text{Intercept} = \Delta S /R \quad (8)$$

Table 3 Effect of temperature on equilibrium constant for the adsorption of Zn^{2+} ions in regenerated CoMo/γ Al_2O_3 catalysts.

Temperature (K)	**1/T, K^{-1}**	**C_e (mg/L)**	**Q_e (mg/g)**	**K**	**ln k**
298	0.00335	0.2266	41.5722	440.3057	6.0874
308	0.00324	6.1880	39.0883	15.1602	2.7186
318	0.00314	7.9727	38.3447	11.5428	2.4460
328	0.00304	8.3132	38.2028	11.0290	2.4005
338	0.00295	8.6188	38.0755	10.6025	2.3610

Figure 9 shows a high linear correlation in the Van't Hoff plot, which gives a strong mathematical basis for the breakdown of the system's thermodynamic profile. The positive slope of the plot is unique to the inverse correlation between the computed equilibrium constant (ln K) and the temperature (T) that agrees with the reduced removal efficiency at elevated temperatures. From a thermodynamic point of view, the positive slope ($-\Delta H^o/R$) of the plot experimentally indicates that the ΔH^o is mathematically negative ($\Delta H^o < 0$), which essentially confirms the exothermic nature of Zn^{2+} immobilization onto the regenerated CoMo/γ-Al_2O_3 matrix. Concurrently, the negative Y-intercept induces a negative standard entropy change ($\Delta S^o < 0$) that unveils a localized loss of degrees of freedom and molecular randomness at the solid-liquid interface, as solvated divalent zinc ions transition from a chaotic bulk solution to a more ordered state upon state-specific surface fixation.

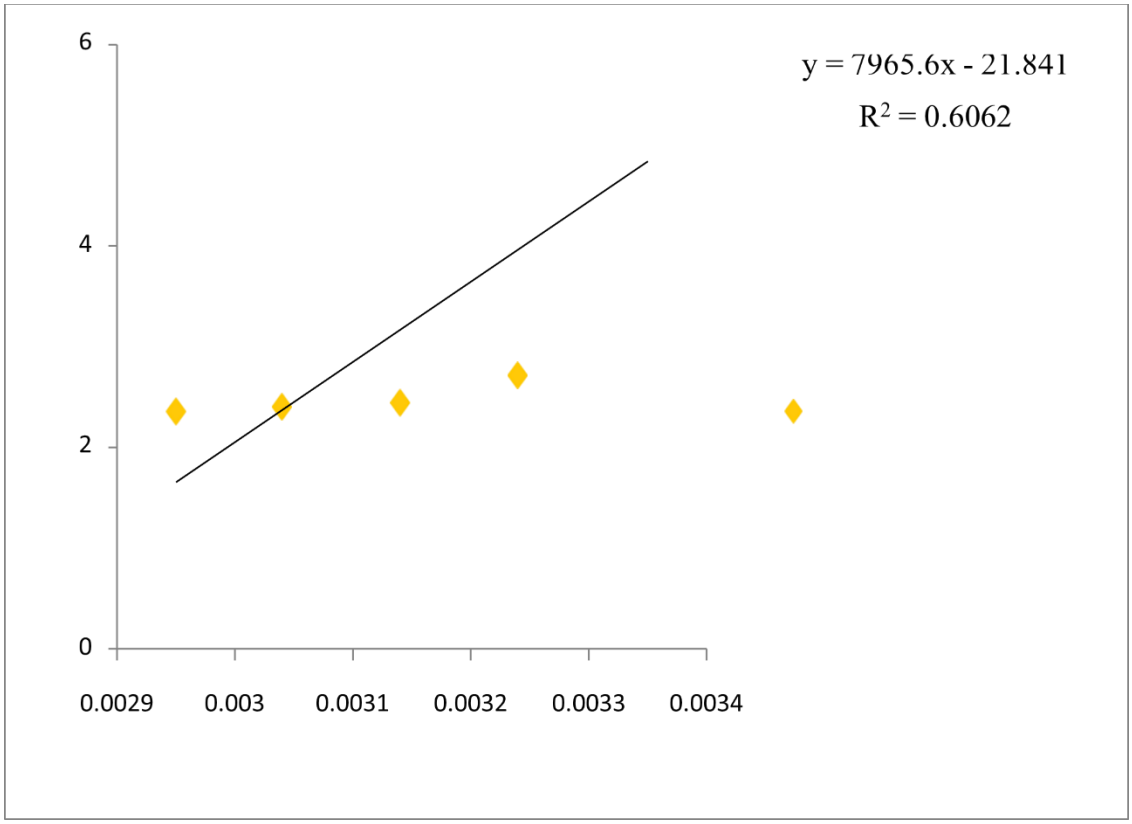

Figure 9 Van 't Hoff Plot for adsorption of Zn^{2+} ions on regenerated CoMo/γ-Al_2O_3 catalyst.

The thermodynamic functions of ΔGº, ΔHº, and ΔSº are listed in Table 4. Negative values of ΔGº at all the examined temperatures have proved that the adsorption is feasible and spontaneous. Moreover, the negative value of ΔHº indicates that the adsorption process is exothermic [72]. Finally, the negative value of ΔSº shows a reduction in randomness at the solid-solution interface.

Table 4 Values of thermodynamic functions for the adsorption of Zn^{2+} on the regenerated CoMo/γ-Al_2O_3 catalyst at different temperatures.

Temperature (K)	**ΔGº (KJ/mol)**	**ΔHº (KJ/mol)**	**ΔSº (J/mol.K)**
298	-15.0819	-66.2259	-181.5860
308	-6.9615		
318	-6.4670		
328	-6.5462		
338	-6.6349		

4. CONCLUSIONS

This work successfully regenerated the spent CoMo/γ-Al_2O_3 hydrodesulfurization catalyst and repurposed it to serve as an adsorbent for zinc ions removal from water samples. n-hexane extraction, oxalic acid treatment, and calcination removed all the coke, foulants, and carbonaceous materials in the catalyst and resulted in improved surface properties. The characterization data confirmed the recovery of catalyst structure, where XRD data indicated nanocrystallinity and crystallites averaging 2.0283 nm, and BET analysis confirmed the high surface area value of 189.13 m^2/g with mesoporous structure. In addition, the regeneration procedure resulted in increased adsorption capacity for zinc ions removal to a rate of 99.77%, compared to 59% from the spent catalyst. It took 30 min for the adsorption equilibrium to be established, and this was influenced by parameters such as contact time, amount of adsorbent, initial zinc ion concentration, and temperature. At optimum conditions, the adsorption capacity was 557.50 mg/g. From thermodynamics evaluation, the adsorption process was spontaneous, exothermic, and involved decreased randomness at solid-solution interface.

References

[1] A. M. A. Al-Lami, S. R. Khudhaier, O. A. Aswad, A. M. A. Al-Lami, Annals of Tropical Medicine and Public Health 23 (2020) SP231125 https://doi.org/10.36295/ASRO.2020.231125
[2] E. B. Hussein, F. A. Rasheed, A. S. Mohammed, K. F. Kayani, RSC Advances 15 (2025) 41061 https://doi.org/10.1039/D5RA06914A
[3] S. A. M. Ealia, M. P. Saravanakumar, IOP Conference Series: Materials Science and Engineering 263 (2017) 032019 https://doi.org/10.1088/1757-899X/263/3/032019
[4] A. Q. Tuama, G. A. Fadhil, W. A. S. Al-dulaimi, Experimental and Theoretical Nanotechnology 10 (2026) 25 https://doi.org/10.56053/10.1.25
[5] S. Baruah, M. N. Khan, J. Dutta, Environmental Chemistry Letters 14 (2016) 1 https://doi.org/10.1007/s10311-015-0542-2
[6] I. Tlili, T. A. Alkanhal, Journal of Water Reuse and Desalination 9 (2019) 232 https://doi.org/10.2166/wrd.2019.057
[7] S. Kumar, W. Ahlawat, G. Bhanjana, S. Heydarifard, M. M. Nazhad, N. Dilbaghi, Journal of Nanoscience and Nanotechnology 14 (2014) 1838 https://doi.org/10.1166/jnn.2014.9050
[8] T. E. Oladimeji, M. Oyedemi, M. E. Emetere, O. Agboola, J. B. Adeoye, O. A. Odunlami, Heliyon 10 (2024) e40370 https://doi.org/10.1016/j.heliyon.2024.e40370
[9] C. M. Park, D. Wang, J. Han, J. Heo, C. Su, Applied Surface Science 471 (2019) 8 https://doi.org/10.1016/j.apsusc.2018.11.240
[10] Hasan M. Azeez, Dalila Elhmaidi, Osama T. Al-Taai, Experimental and Theoretical NANOTECHNOLOGY, 10 (2026) 47 https://doi.org/10.56053/10.1.47
[11] S. Meftah, K. Meftah, M. Drissi et al., Discover Sustainability 6 (2025) 137 doi:10.1007/s43621-025-00895-6
[12] C. F. Carolin, P. S. Kumar, A. Saravanan, G. J. Joshiba, M. Naushad, Journal of Environmental Chemical Engineering 5 (2017) 2782 https://doi.org/10.1016/j.jece.2017.05.029
[13] A. Alengebawy, S. T. Abdelkhalek, S. R. Qureshi, M.-Q. Wang, Toxics 9 (2021) 42 https://doi.org/10.3390/toxics9030042
[14] Ali Abdull Haleem, Manal Midhat Abdullah, Experimental and Theoretical NANOTECHNOLOGY, 10 (2026) 93 https://doi.org/10.56053/10.1.93
[15] A. I. Chowdhury, L. C. Shill, M. M. Raihan, R. Rashid, M. N. H. Bhuiyan, S. Reza, M. R. Alam, Scientific Reports 14 (2024) 15616 https://doi.org/10.1038/s41598-024-65734-6

[16] J. N. Ihedioha, P. O. Ukoha, N. R. Ekere, Environmental Geochemistry and Health 39 (2017) 497 https://doi.org/10.1007/s10653-016-9830-4
[17] P. J. Alegbe, M. Appiah-Brempong, E. Awuah, Scientific African 27 (2025) e02603 https://doi.org/10.1016/j.sciaf.2025.e02603
[18] P. Wongsasuluk, S. Chotpantarat, W. Siriwong, M. Robson, Environmental Geochemistry and Health 36 (2014) 169 https://doi.org/10.1007/s10653-013-9537-8
[19] Q. Chen, Y. Yao, X. Li, J. Lu, J. Zhou, Z. Huang, Journal of Water Process Engineering 26 (2018) 289 https://doi.org/10.1016/j.jwpe.2018.11.003
[20] S. Bolisetty, M. Peydayesh, R. Mezzenga, Chemical Society Reviews 48 (2019) 463 https://doi.org/ 10.1039/C8CS00493E
[21] A. E. Burakov, E. V. Galunin, I. V. Burakova, A. E. Kucherova, S. Agarwal, A. G. Tkachev, V. K. Gupta, Ecotoxicology and Environmental Safety 148 (2018) 702 https://doi.org/10.1016/j.ecoenv.2017.11.034
[22] G. Crini, E. Lichtfouse, L. D. Wilson, N. Morin-Crini, Environmental Chemistry Letters 17 (2019) 195 https://doi.org/10.1007/s10311-018-0786-8
[23] I. Ali, V. K. Gupta, Nature Protocols 1 (2006) 2661 https://doi.org/10.1038/nprot.2006.370
[24] P. N. Dave, L. V. Chopda, Journal of Nanotechnology 2014 (2014) 398569 https://doi.org/10.1155/2014/398569
[25] Ali Maher alshammari, Tagreed K Hamad, Alaa Jabbar Ghazai, Mohamed Dammak, Experimental and Theoretical NANOTECHNOLOGY, 10 (2026) 131 https://doi.org/10.56053/10.1.131
[26] H. N. Tran, S.-J. You, A. Hosseini-Bandegharaei, H.-P. Chao, Water Research 120 (2017) 88–116 https://doi.org/10.1016/j.watres.2017.04.014
[27] J. Wang, X. Guo, Journal of Hazardous Materials 390 (2020) 122156 https://doi.org/10.1016/j.jhazmat.2020.122156
[28] S. S. Ba Hashwan, M. H. M. Khir, I. M. Nawi, M. A. Hassan, A. S. Algamili, H. Shutari, Experimental and Theoretical Nanotechnology 9 (2025) 539 https://doi.org/10.56053/9.4.539
[29] Z. Raji, A. Karim, A. Karam, S. Khalloufi, Waste 1 (2023) 775 https://doi.org/10.3390/waste1030046
[30] F. Gomri, G. Finqueneisel, T. Zimny, S. A. Korili, A. Gil, M. Boutahala, Applied Water Science 8 (2018) 164 https://doi.org/10.1007/s13201-018-0823-6
[31] F. B. Vasheghani, F. H. Rajabi, M. H. Omidi, S. Shabanian, Russian Journal of Physical Chemistry A 89 (2015) 876 https://doi.org/10.1134/S0036024415050337
[32] H. N. Tran, N. P. Thanh Trung, E. C. Lima, J.-C. Bollinger, N. D. Dat, H.-P. Chao, R.-S. Juang, Journal of Chemical Technology and Biotechnology 98 (2023) 462 https://doi.org/10.1002/jctb.7258
[33] E. C. Lima, A. Hosseini-Bandegharaei, J. C. Moreno-Piraján, I. Anastopoulos, Journal of Molecular Liquids 273 (2019) 425 https://doi.org/10.1016/j.molliq.2018.10.048
[34] M. S. Akhtar, S. Ali, W. Zaman, Catalysts 14 (2024) 841 https://doi.org/10.3390/catal14120841
[35] L. Zhao, X. Zhang, Z. Tan, G. Jiang, Y. Chen, D. Pan, Science of The Total Environment 953 (2024) 176127 https://doi.org/10.1016/j.scitotenv.2024.176127
[36] X. L. Wang, Z. Zhao, Z. T. Chen, J. M. Li, A. J. Duan, C. M. Xu, D. W. Gao, Z. W. Cao, P. Zheng, J. Y. Fan, Fuel Processing Technology 161 (2017) 52 https://doi.org/10.1016/j.fuproc.2017.03.003
[37] I. Shafiq, S. Shafique, P. Akhter, W. Yang, M. Hussain, Catalysis Reviews: Science and Engineering 64 (2022) 1 https://doi.org/10.1080/01614940.2020.1780824
[38] H. Liu, Y. Li, C. Yin, Y. Wu, Y. Chai, D. Dong, X. Li, C. Liu, Applied Catalysis B: Environmental 198 (2016) 493 https://doi.org/10.1016/j.apcatb.2016.06.004

[39] X. Wang, Z. Zhao, P. Zheng, Z. Chen, A. Duan, C. Xu, J. Jiao, H. Zhang, Z. Cao, B. Ge, Journal of Catalysis 344 (2016) 680 https://doi.org/10.1016/j.jcat.2016.10.016
[40] Fatimah Nameer Shaban, Marwa Jewi, Experimental and Theoretical NANOTECHNOLOGY, 10 (2026) 165 https://doi.org/10.56053/10.S.165
[41] Fatima J Musaa, Hanaa J. Kadhim Alesa, Experimental and Theoretical NANOTECHNOLOGY, 10 (2026) 197 https://doi.org/10.56053/10.S.197
[42] A. Pimerzin, A. Roganov, A. Mozhaev, K. Maslakov, P. Nikulshin, A. Pimerzin, Fuel Processing Technology 173 (2018) 56 https://doi.org/10.1016/j.fuproc.2018.01.008
[43] C. Leyva, J. Ancheyta, L. Mariey, A. Travert, F. Maugé, Catalysis Today 220 (2014) 89 https://doi.org/10.1016/j.cattod.2013.10.007
[44] P. T. H. Pham, C. Q. Pham, T.-T. Dam, Q.-A. Nguyen, T. M. Nguyen, Fuel Processing Technology 265 (2025) 108170 https://doi.org/10.1016/j.fuproc.2024.108170
[45] M. Marafi, A. Stanislaus, Industrial & Engineering Chemistry Research 50 (2011) 9495 https://doi.org/10.1021/ie200789u
[46] M. Marafi, A. Stanislaus, Resources, Conservation and Recycling 53 (2008) 1 https://doi.org/10.1016/j.resconrec.2008.08.005
[47] B. Singh, Journal of Hazardous Materials 167 (2009) 24 https://doi.org/10.1016/j.jhazmat.2009.01.071
[48] E. Furimsky, F. E. Massoth, Catalysis Today 52 (1999) 381 https://doi.org/10.1016/S0920-5861(99)00096-6
[49] Raghda S. Al-Awadi, Sundus A. Abdullah, Osama T. Al-Taai, Experimental and Theoretical NANOTECHNOLOGY, 10 (2026) 219 https://doi.org/10.56053/10.S.219
[50] R. Karthik, S. Meenakshi, Chemical Engineering Journal 263 (2015) 168 https://doi.org/10.1016/j.cej.2014.11.015
[51] Z. Abbas, S. M. Jung, PLoS ONE 19 (2024) e0296271 https://doi.org/10.1371/journal.pone.0296271
[52] S.-Y. Ahn, W.-J. Na, K.-J. Kim, B.-J. Kim, H.-K. Park, H.-S. Roh, Catalysts 13 (2023) 738 https://doi.org/10.3390/catal13040738
[53] M. Tian, H. Liu, J. Cui, Y. Weng, X. Wang, E. Feng, W. Zhang, C. Cao, J. Wen, G. Huang, S. Xu, Journal of Hazardous Materials 472 (2024) 134514 https://doi.org/10.1016/j.jhazmat.2024.134514
[54] Y. J. O. Asencios, M. R. Sun-Kou, Applied Surface Science 258 (2012) 10002 https://doi.org/10.1016/j.apsusc.2012.06.063
[55] Y. B. Onundi, A. A. Mamun, M. F. Al Khatib, Y. M. Ahmed, International Journal of Environmental Science & Technology 7 (2010) 751 https://doi.org/10.1007/BF03326184
[56] M. Ahamed, H. A. Alhadlaq, M. A. M. Khan, P. Karuppiah, N. A. Al-Dhabi, Journal of Nanomaterials 2014 (2014) 637858 https://doi.org/10.1155/2014/637858
[57] M. R. Karim, M. A. Rahman, M. A. J. Miah, H. Ahmad, M. Yanagisawa, M. Ito, Open Colloid Science Journal 4 (2011) 32 https://doi.org/10.2174/1876530001104010032
[58] A. A. Asadi, S. M. Alavi, S. J. Royaee, M. Bazmi, Energy & Fuels 32 (2018) 2203 https://doi.org/10.1021/acs.energyfuels.7b03461
[59] N. Topnani, S. Kushwaha, T. Athar, International Journal of Green Nanotechnology: Materials Science & Engineering 1 (2010) 67 https://doi.org/10.1080/19430840903430220
[60] M. Maruthupandy, Y. Zuo, J. S. Chen, J. M. Song, H. L. Niu, C. J. Mao, S. Y. Zhang, Y. H. Shen, Applied Surface Science 397 (2017) 167 https://doi.org/10.1016/j.apsusc.2016.11.118
[61] A. A. Farghali, M. Bahgat, A. E. Allah, M. H. Khedr, Beni-Suef University Journal of Basic and Applied Sciences 2 (2013) 61 https://doi.org/10.1016/j.bjbas.2013.01.001
[62] S. K. Khaja Muswareen, K. Venkatarao, S. Cole, Physical Chemistry Research 11 (2023) 241 https://doi.org/10.22036/PCR.2022.337333.2077

[63] U. Zafar, M. A. Bhatti, A. Akram, Pakistan Journal of Analytical and Environmental Chemistry 19 (2018) 53 https://doi.org/10.21743/pjaec/2018.06.05
[64] G. Akkaya, F. Güzel, Journal of Dispersion Science and Technology 34 (2013) 1295 https://doi.org/10.1080/01932691.2012.743863
[65] A. A. Al-Homaidan, A. F. Al-Abbad, A. A. Al-Hazzani, A. A. Al-Ghanayem, J. A. Alabdullatif, International Journal of Phytoremediation 18 (2016) 184 https://doi.org/10.1080/15226514.2015.1073673
[66] R. Ahmad, A. Mirza, Journal of Molecular Liquids 249 (2018) 805 https://doi.org/10.1016/j.molliq.2017.11.082
[67] M. Tazik, M. H. Dehghani, K. Yaghmaeian, S. Nazmara, M. Salari, A. H. Mahvi, S. Nasseri, H. Soleimani, R. R. Karri, Scientific Reports 13 (2023) 8503 https://doi.org/10.1038/s41598-023-35117-4
[68] M. Marafi, A. Stanislaus, Journal of Hazardous Materials 101 (2003) 123 https://doi.org/10.1016/S0304-3894(03)00145-6
[69] K. S. Shabani, F. D. Ardejani, K. Badii, M. E. Olya, Arabian Journal of Chemistry 10 (2017) S3108 https://doi.org/10.1016/j.arabjc.2013.12.001
[70] M. M. Youssif, A. El-Naggar, M. Abd El-Aziz, A. M. Elgarahy, Materials 17 (2024) 5141 https://doi.org/10.3390/ma17215141
[71] M. A. Atieh, O. Y. Bakather, B. S. Tawabini, A. A. Bukhari, M. Khaled, M. Alharthi, M. Fettouhi, F. A. Abuilaiwi, Journal of Nanomaterials 2010 (2010) 232378 https://doi.org/10.1155/2010/232378
[72] M. Verma, I. Tyagi, R. Chandra, V. K. Gupta, Journal of Molecular Liquids 225 (2017) 936 https://doi.org/10.1016/j.molliq.2016.04.045